[13] M. J. Janssen, J. G. A. Luitjen, and G. J. M. Van der Kerk, Rec. Trav. Chim. **82,** 90 (1963); R. E. Hester, J. Organometal. Chem. **23,** 123 (1970).
[14] For a detailed tabulation of reported Mössbauer data, see J. J. Zuckerman, Advan. Organometal. Chem. **9,** 21 (1970). See also Refs. 9 and 12, above.
[15] H. C. Clark, R. J. O'Brien, and J. Trotter, Proc. Chem. Soc. (London) **1963,** 85; J. Chem. Soc. **1964,** 2332.
[16] R. H. Herber and S. C. Chandra, J. Chem. Phys. **54,** 1847 (1971).
[17] E. O. Schlemper and W. C. Hamilton, Inorg. Chem. **5,** 995 (1966).
[18] R. H. Herber and S. Chandra, J. Chem. Phys. **52,** 6045 (1970).
[19] The I.S. and Q.S. values for $Bu_2Sn(OAc)_2$ previously reported[20] are 1.40±0.10 and 3.45±0.10 mm/sec and[21] 1.34±0.08 and 3.50±0.08 mm/sec both sets at liquid-nitrogen temperature. The present data, summarized in Table I, obtained with a narrow-line source, are regarded as somewhat more precise (and well within the error limits of the earlier data).
[20] A. Yu. Aleksandrov, N. N. Delyagin, K. P. Mitrofanov, L. S. Polak, and V. S. Shpinel', Dokl. Akad. Nauk SSSR **148,** 126 (1963).
[21] V. I. Gol'danskii, E. F. Makarov, R. A. Stukan, V. A. Trukhtanov, and V. V. Khrapov, Dokl. Akad. Nauk SSSR **151,** 357 (1963).
[22] S. L. Ruby and P. A. Flinn, Rev. Mod. Phys. **36,** 351 (1964); R. L. Collins, J. Chem. Phys. **42,** 1072 (1965).

THE JOURNAL OF CHEMICAL PHYSICS VOLUME 54, NUMBER 9 1 MAY 1971

Electron Paramagnetic Resonance and Optical Spectra of Pentacyanocobaltate(II)

FUN-DOW TSAY AND HARRY B. GRAY
Arthur Amos Noyes Laboratory of Chemical Physics, California Institute of Technology, Pasadena, California 91109*
AND
J. DANON
Centro Brasileiro de Pesquisas Fisicas, Rio de Janeiro, Brazil
(Received 26 August 1970)

Electron paramagnetic resonance (EPR) and optical spectral studies have been carried out on the pentacyanocobaltate(II) ion in ethylene glycol–water solutions, and in electron-irradiated powder samples of $K_3Co(CN)_6$. Both EPR and optical spectra observed for the ion in the powder samples are essentially similar to those obtained from the ethylene glycol–water solutions. There was no observable linewidth variation with nuclear spin states M_I, no dependence on the different solvent media used, and no dependence on the concentration ratio Co^{2+}/CN^-, in both X-band and K-band spectra. The results indicate that the structure of $Co(CN)_5^{3-}$ in solutions and in polycrystalline media is a slightly distorted square pyramid with no solvent bound in the sixth coordination site. The two strong hyperfine components with exceptionally large spacings occurring at the low-field end of the X-band spectrum are identified as the so-called angular anomalies. An effective method of simulation of the first-derivative EPR spectra of polycrystalline samples has also been developed.

INTRODUCTION

The molecular and electronic structure of pentacyanocobaltate(II) ion in liquid solutions has been the subject of several paramagnetic resonance and optical spectral studies.[1–4] Although its structure, based largely on electron paramagnetic resonance (EPR) data, has been suggested to be square pyramidal (C_{4v} symmetry) with the unpaired electron in an $a_1(d_{z^2})$ orbital, there remains some speculation concerning the existence of a solvated six-coordinate species, $[Co(CN)_5H_2O]^{3-}$. The solvated complex would be expected to have essentially the same ground electronic configuration as determined in the case of $Co(CN)_5^{3-}$.

Recent EPR studies have suggested that the pentacyanocobaltate(II) ion is solely responsible for the paramagnetic resonance observed in a single crystal of $K_3Co(CN)_6$ subjected to either electron[5] or x-ray[6] bombardment and in powder samples of thermally decomposed $K_6Co_2(CN)_{12}$.[7] The differences in the reported EPR data for $Co(CN)_5^{3-}$ could indicate the importance of a specific interaction in the available axial coordination site. More likely, however, the minor discrepancies may simply reflect the problems inherent in analyzing spectra taken for crystal and polycrystalline samples, in view of the lower than axial symmetry that the central metal ion possesses in a single crystal of $K_3Co(CN)_6$, and the fact that two magnetically different sites are present in a unit cell.[8]

In an attempt to clarify the structural situation, we have carefully analyzed the X-band and K-band EPR and the optical spectra of $Co(CN)_5^{3-}$ in ethylene glycol–water solutions and in electron-irradiated $K_3Co(CN)_6$ powder samples. A method for simulating the first-derivative EPR line shape of powder or frozen glass samples containing axially symmetrical $S=\frac{1}{2}$ transition metal complexes has been developed in conjunction with this effort. This method, which does not require tedious calculations of the absorption intensity, is particularly effective in cases such as $Co(CN)_5^{3-}$ where the so-called[9] angular anomalies occur.

EXPERIMENTAL

Electron paramagnetic resonance spectra were obtained with a Varian V-4500 spectrometer operating at X-band (9.432 GHz) and K-band frequencies (34.88 GHz) using 100 KHz field modulation. The magnetic field was measured with an Alpha Model 675 NMR gaussmeter. The g values were obtained both by calculation from the cavity frequency and the resonance magnetic field, and by comparison with the resonance position of a 0.1% DPPH($g=2.0037$) dispersed in solid KCl. The two methods yield g values in agreement within 0.03%. For the work at low temperature, precooled nitrogen gas was blown through the cavity whose temperature was then controlled by regulating the flow rate of the nitrogen gas using a Varian Model V-4540 variable temperature controller plus accessories. Maximum flow rate was used for the measurement near 77°K. All samples were sealed under vacuum in 3-mm-o.d., and 1-mm-o.d. quartz tubes, respectively, for X-band and K-band measurements. Optical spectra were obtained with a Cary Model 14 CMRI spectrophotometer equipped with a Cary diffuse reflectance accessory.

The electron irradiation of the samples of $K_3Co(CN)_6$ was made at 77°K using the 2-MeV linear accelerator of the Centro Brasileiro de Pesquisas Físicas, Rio de Janeiro, Brazil. Measurements were carried out on a single crystal which had been irradiated at 10 μA for 4 min, and on the powders irradiated at 5 μA for various lengths of time up to 5 min. The samples exhibited a light brown color after irradiation.

Samples with varying concentration ratios of CN^-/Co^{2+} were prepared under high vacuum (10^{-5} torr) in deoxygenated ethylene glycol–water solutions (2:1 V/V mixture). In a typical preparation, a solution of 52.1 mg (0.80 mmoles) KCN in 1 ml of ethylene glycol–water was used to dissolve 29.2 mg (0.10 mM) $Co(NO_3)_2\cdot 6H_2O$. A small portion of the clear solution was then transferred under vacuum into a quartz sample tube for EPR measurements.

EPR LINE-SHAPE CALCULATIONS

Many attempts have been made in recent years[10] to calculate the EPR spectra of powder or frozen glass samples containing axially symmetric $S=\frac{1}{2}$ transition metal complexes. Although many of these calculations have involved computer simulation techniques,[11] and subsequent treatments have been extended to include line-shape functions,[12] angular anomalies,[9] rhombic distortions,[13] and quadrupole effects,[14] the method for calculation is still based on the interpretation of the polycrystalline spectrum first suggested by Sands.[15] As a result, most of these calculations are involved in one form or other with calculating the absorption intensity as a function of resonance field before taking the first derivative of the absorption line. Since both resonance field position and absorption intensity are not simple analytical functions of θ (the angle between the external magnetic field and the symmetry axis of the molecule), an explicit expression for the absorption intensity as a function of resonance field cannot be obtained without making some tedious numerical calculations and several serious approximations.[16] This situation becomes more critical, in particular, when a large anisotropy is present in the nuclear hyperfine interaction.[9,14] It will be demonstrated in this section that simulations of the first derivative EPR line shape (based on a useful relationship that exists between the resonance field position and its absorption intensity) can be performed without resort to lengthy calculations of the absorption intensity.

For $S=\frac{1}{2}$ transition metal complexes with nuclear spin I and axial symmetry, the spin-Hamiltonian has been given as[17]

$$\mathcal{H}=g_{||}\beta H_r S_r+g_\perp\beta(H_pS_p+H_qS_q)+A\,S_rI_r +B(S_pI_p+S_qI_q)+Q'\{I_r^2-\tfrac{1}{3}I(I+1)\} -g_N\beta_N H\cdot\hat{I}, \quad (1)$$

where r, p, and q refer to the coordinates of the molecule with the symmetry axis in the r direction. The electron g values parallel and perpendicular to the symmetry axis are given as $g_{||}$ and $g_\perp$, respectively, and g_N is the nuclear g value; β and β_N are the Bohr and nuclear magnetons. The nuclear hyperfine coupling constants parallel and perpendicular to the symmetry axis r are given, respectively, as A and B. Q' is the nuclear electric quadrupole coupling constant, $H_{r,p,q}$ are the components of the magnetic field vector, and $\hat{S}$ and $\hat{I}$ represent the electron and nuclear spin angular momentum operators.

When a transformation is made from the molecular axes (r, p, q) into the laboratory frame (x, y, z) with the applied external magnetic field H along the z direction, one obtains

$$\begin{aligned}\mathcal{H}=&g\beta HS_z+KS_zI_z+\tfrac{1}{4}B[(A/K)-1](S_+I_++S_-I_-)\\&+\tfrac{1}{4}B[(A/K)+1](S_+I_-+S_-I_+)\\&+\frac{(B^2-A^2)g_{||}g_\perp\sin\theta\cos\theta}{2Kg^2}[(S_++S_-)I_z+S_z(I_++I_-)]\\&+\tfrac{1}{2}Q'[I_z^2-\tfrac{1}{3}(I+1)][(3A^2g_{||}^2\cos^2\theta/K^2g^2)-1]\\&+\tfrac{1}{4}Q'[I_+^2+I_-^2](B^2g_\perp^2/K^2g^2)\sin^2\theta\\&-\frac{Q'}{2}[I_z(I_++I_-)+(I_++I_-)I_z]\left(\frac{ABg_{||}g_\perp}{K^2g^2}\right)\sin\theta\cos\theta\\&-g_N\beta_NH\left[\frac{(Ag_{||}\cos^2\theta+Bg_\perp\sin^2\theta)I_z}{Kg}\right.\\&\left.+\frac{(Ag_{||}-Bg_\perp)\sin\theta\cos\theta}{2Kg}(I_++I_-)\right], \quad (2)\end{aligned}$$

where

$$g^2=g_{||}^2\cos^2\theta+g_\perp^2\sin^2\theta, \tag{3}$$

$$K^2g^2=A^2g_{||}^2\cos^2\theta+B^2g_\perp^2\sin^2\theta, \tag{4}$$

$S_\pm=S_x\pm iS_y$, $I_\pm=I_x\pm iI_y$, and θ is the angle between the applied external magnetic field and the symmetry axis of the molecule. From these expressions, the resonance field for the allowed ($\Delta M_S=\pm1$, $\Delta M_I=0$), and forbidden ($\Delta M_S=\pm1$, $\Delta M_I=\pm1, \pm2$) transitions can be obtained. Since quadrupole effects, which are known to contribute to the intensities of transitions with $\Delta M_I>0$, and which cause the resonance field positions for both allowed and forbidden transitions to shift, are found to be insignificant in the ion under study here, we therefore have made no effort in our present treatment to include these effects. However, the method given below could be extended to apply to such a situation.

From Eq. (2), the angular dependence of the resonance field for the allowed transitions ($\Delta M_S=\pm1$, $\Delta M_I=0$), including second-order hyperfine interaction, can be expressed as follows[18]:

$$H(\theta, M_I)=\frac{h\nu^0}{g\beta}-\frac{KM_I}{g\beta}$$
$$-\frac{B^2}{4g^2\beta^2H^0}\left(\frac{A^2+K^2}{K^2}\right)[I(I+1)-M_I^2]$$
$$-(2g^2\beta^2H^0)^{-1}\left(\frac{A^2-B^2}{K}\right)^2\left(\frac{g_{||}g_\perp}{g^2}\right)^2\sin^2\theta\cos^2\theta M_I^2, \tag{5}$$

where $H^0=h\nu^0/g\beta$. A similar equation with all coupling constants expressed in units of gauss, including quadrupole effects, has been derived by Rollmann and Chan,[14] and the resonance field for the forbidden transitions has also been given in their paper.

In powder or frozen glass samples, all orientations are equally probable for a molecule with its symmetry axis making an angle θ with respect to the applied external magnetic field. Since the number of molecules which orient between θ and $\theta+d\theta$ is known[15] to be proportional to $\frac{1}{2}\sin\theta d\theta$ at the resonance field between H and $H+dH$, the absorption intensity thus becomes[9,15]

$$\frac{dN}{dH}=\tfrac{1}{2}N_0\sin\theta\left(\frac{d\theta}{dH}\right)=\frac{N_0\sin\theta}{2(dH/d\theta)}, \tag{6}$$

where N_0 is the total number of molecules. The rate of change of the resonance field H with angle θ, $(dH/d\theta)$, can be calculated from Eqs. (3)–(5), which then yields the following expression:

$$\frac{dH}{d\theta}=\frac{\sin\theta\cos\theta}{g^2}\left[(g_{||}^2-g_\perp^2)H^0\right.$$
$$\left.+\frac{M_I}{g\beta}\left(\frac{A^2g_{||}^2-B^2g_\perp^2}{K}+2K(g_\perp^2-g_{||}^2)\right)\right]. \tag{7}$$

On substituting Eq. (7) into Eq. (6), one obtains

$$\frac{dN}{dH}=\left(\frac{N_0g^2}{2\cos\theta}\right)\left[(g_{||}^2-g_\perp^2)H^0\right.$$
$$\left.+\frac{M_I}{g\beta}\left(\frac{A^2g_{||}^2-B^2g_\perp^2}{K}+2K(g_\perp^2-g_{||}^2)\right)\right]^{-1}. \tag{8}$$

From Eq. (8) it can be seen that the absorption intensity becomes infinity at $\theta=90°$, and at an arbitrary angle where the quantity in the brackets [ ] approaches zero. The latter situation is the so-called extra absorption or the angular anomaly.[10] Experimentally, the only resonance peaks that can be observed in a polycrystalline EPR spectrum fall in the regions where $(dH/d\theta)\to0$. This is anticipated from the relationship between (dN/dH) and $(dH/d\theta)$ as described in Eqs. (6) and (8), except it is not obvious that a resonance peak should also occur in the g-parallel region ($\theta=0°$) where from the population factor $\frac{1}{2}\sin\theta$ alone it is expected to have minimum intensity. However, from the characteristics of sine and cosine functions that are involved in the expression for the angularly dependent resonance field $H(\theta, M_I)$[Eq. (5)], the rate of change of $H(\theta, M_I)$ with angle θ is expected to be much slower near the regions where $(dH/d\theta)\to0$ than any other regions. Physically, this means that although molecules may orient at slightly different angles in the region where $(dH/d\theta)\to0$, their resonance field will change the least. As a result, contributions to the absorption intensity from those individual molecules in this region become much more significant than those in the other region. Based on this finding, the first-derivative EPR line shape for the polycrystalline samples can be calculated directly by computing the following amplitude:

$$\sum_\theta\sum_{M_I}S'[H-H(\theta, M_I)]p(\theta, M_I)\sin\theta, \tag{9}$$

where $S'[H-H(\theta, M_I)]$ is the first derivative Lorentzian or Gaussian line shape function, and $H(\theta, M_I)$ is the resonance field for all transitions, which can be obtained from Eq. (5) in the present case involving only the allowed transition. The transition probability is represented by $P(\theta, M_I)$, in which the angular dependence for the allowed transition is usually negligible.[9,19] The factor $\sin\theta$ is also included in Eq. (9) to account for the angular dependence of the number of molecules. The advantages of this approach become apparent when compared with the standard method of calculating the first-derivative line shape (d^2N/dH^2) after obtaining the absorption intensity (dN/dH). First of all, there is no need for the calculations of (dN/dH) as a function of $H(\theta, M_I)$ in the present treatment. As can be seen from Eqs. (5) and (8), it is tedious to express (dN/dH) as a function of H, and almost impossible to obtain the first derivative in the form of (d^2N/dH^2), except through numerical

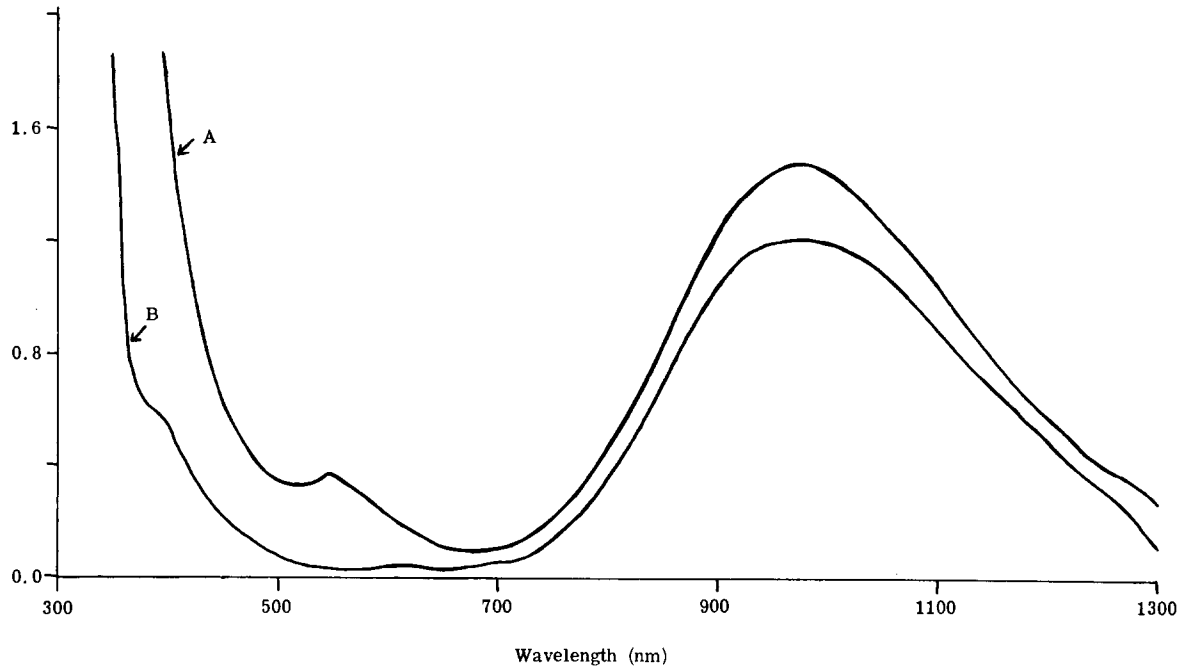

FIG. 1. Optical spectra of pentacyanocobaltate(II): *A*, in electron-irradiated $K_3Co(CN)_6$ crystal; and *B*, in ethylene glycol–water (2:1) solutions.

calculations. Secondly, in the present approach, no adjustments have to be made for those absorption intensities (dN/dH) which are expected to become infinite at $\theta=90°$ and at angular anomalies; in particular, in the latter case, the absorption intensity may even change sign after it reaches infinity. Adjustments for the infinite intensities made the standard (dN/dH) calculation impractical and inaccurate.

A FORTRAN IV program written for the IBM 360/75 computer has been developed to simulate the first-derivative line shape of the X-band and K-band spectra for the pentacyanocobaltate(II) ions in ethylene glycol–water solutions and in electron-irradiated $K_3Co(CN)_6$ powder samples. The first part of the program was written to calculate the resonance field $H(\theta, M_I)$ from Eq. (5), from which the second part of the program was able to perform the line shape simulations by computing the amplitude from

$$\sum_{\theta}\sum_{M_I}\frac{p(\theta, M_I)[H-H(\theta, M_I)]\Delta\sin\theta}{\{3\Delta^2+[H-H(\theta, M_I)]^2\}^2}, \qquad (10)$$

where the Lorentzian line-shape function was used for each individual line at resonance field $H(\theta, M_I)$ and with Δ equal to half the peak-to-peak linewidth. The transition probability $p(\theta, M_I)$ is proportional to $g_\perp^2[(g_\parallel/g)^2+1]$ for the allowed transitions[19] ($\Delta M_S=\pm1, \Delta M_I=0$). The summation in Eq. (10) was taken over all angles θ from $\theta=0°$ to 90° at 1° intervals, and over all the nuclear spin states M_I ranging from $-\frac{7}{2}$ to $\frac{7}{2}$ for ^{59}Co. The values for the spin-Hamiltonian parameters were determined on the basis of the best fit for the simulated spectra at both X-band and K-band as compared with the experimentally observed spectra.

RESULTS

Optical Spectra

The optical spectra are shown in Fig. 1 as spectra *A* and *B*, respectively, for a crystal of irradiated $K_3Co(CN)_6$, and for an ethylene glycol–water solution containing $Co(CN)_5^{3-}$. The similarity between the two spectra is quite striking, in particular, the band at 977 nm for the crystal as compared with that at 967 nm observed for the solution. In addition, both bands are found to be equally broad, suggesting that the complexes responsible for the optical absorption are essentially identical in both media. The weaker band observed at 548 nm for the crystal is found to be from an *F*-center caused by radiation damage. The intensity of this band can be reduced to a negligible level by heating the crystal at 115°C for 20 min, whereas the other bands remain unaffected after thermal treatment. The diffuse reflectance spectrum observed for the irradiated powder samples is essentially the same as the absorption spectrum observed for the irradiated crystal. In each case, the intensity of the spectrum is found to increase with increasing irradiation time.

Paramagnetic Resonance Spectra

X-band and K-band spectra were obtained at 298 and 77°K for $Co(CN)_5^{3-}$ in powder $K_3Co(CN)_6$

TABLE I. EPR Data for $Co(CN)_6^{3-}$ in powder and solution samples.

	Electron irradiated $K_3Co(CN)_6$ powder		Ethylene glycol–water solution
	298°K	77°K	77°K
$g_{\|\|}$	2.004±0.001	2.004±0.001	2.004±0.001
$g_\perp$	2.163±0.002	2.162±0.002	2.163±0.002
$g_\perp'$	2.158±0.002	2.158±0.002	2.160±0.002
$A\times10^4$, cm^{-1}	82.76±0.94	82.76±0.94	82.76±0.94
$B\times10^4$, cm^{-1}	−23.70±2.0	−25.70±2.0	−28.30±2.0
$B'\times10^4$, cm^{-1}	−26.70±2.0	−27.70±2.0	−28.20±2.0

samples and in ethylene glycol–water solutions. The EPR data listed in Table I were used as the parameters for simulating the spectra. The spectra observed for the powder and frozen glass samples show the resolved nuclear hyperfine components in both the $g_{||}(\theta=0°)$ and $g_\perp(\theta=90°)$ regions. The general features of the spectra are in agreement with those expected for a randomly oriented $S=\frac{1}{2}$ system with axial symmetry and with nuclear spin $I=\frac{7}{2}$.

$K_3Co(CN)_6$ Powder Samples

The X-band spectra observed for the powder samples of $K_3Co(CN)_6$ at 298 and 77°K are shown in Fig. 2 (spectra *A*, *C*). The signal-to-noise ratio for the spectrum at room temperature is very poor because of the low concentration of paramagnetic species in the samples, but the nuclear hyperfine components of cobalt at both $g_{||}$ and $g_\perp$ regions of the spectrum are discernible. The signal level is greatly improved by lowering the temperature, as can be seen from the spectrum obtained at 77°K, where most of the nuclear hyperfine structure is clearly observable. The sharp, strong peak ($g=2.002$) that occurs near 3400 G is identified as arising from the *F*-center caused by radiation damage.

The resonance field for the nuclear hyperfine components can be calculated from Eq. (5), which predicts the following line positions in the *g*-parallel region ($\theta=0°$),

$$H_{||}=H_{||}^0-AM_I-(B^2g_\perp^2/2H_{||}^0g_{||}^2)\{I(I+1)-M_I^2\}, \quad (11)$$

and in the *g*-perpendicular region ($\theta=90°$)

$$H_\perp=H_\perp^0-BM_I-[(A^2g_{||}^2+B^2g_\perp^2)/4H_\perp^0g_\perp^2]\times\{I(I+1)-M_I^2\}, \quad (12)$$

where $H_{||}^0=h\nu^0/g_{||}\beta$, $H_\perp^0=h\nu^0/g_\perp\beta$, and A, B are given in units of gauss. From these expressions, it can be seen that the second-order hyperfine interaction will shift the line positions to lower fields, and, being proportional to $\{I(I+1)-M_I^2\}$, will cause them to shift asymmetrically. As a result, the spacing between two neighboring hyperfine components is expected to be narrower at lower field. This has been observed in the spectra shown in Fig. 2, except for the two perpendicular hyperfine components that occur at the low-field end of the spectrum, whose spacings of 40 and 26 G are too large to be accounted for as arising from the effect by including the second-order hyperfine interaction. Based on the values given in Table I, it is estimated that the second-order effect should not contribute more than 5 G to the spacing between any two adjacent hyperfine components. Therefore, the

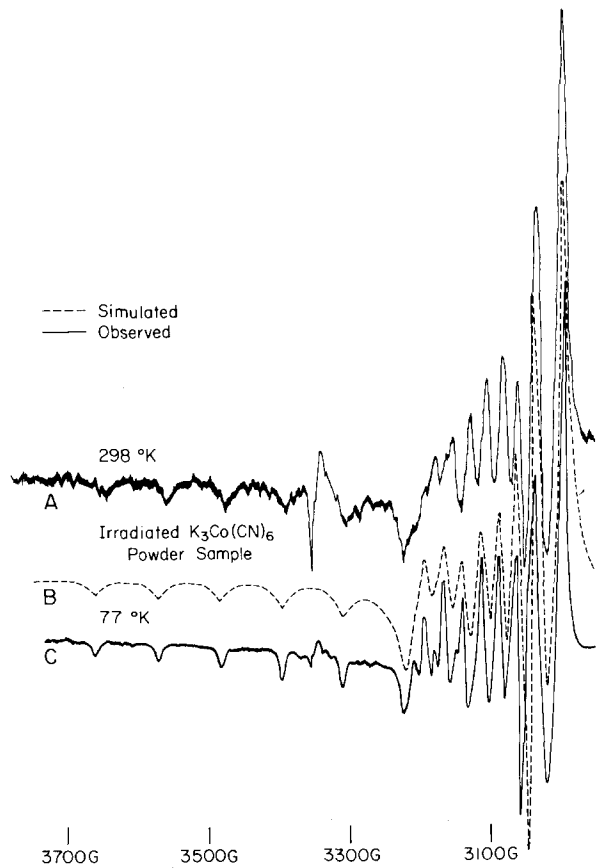

FIG. 2. X-band EPR spectra of pentacyanocobaltate(II) in electron-irradiated $K_3Co(CN)_6$ powder samples: *A*, observed at 298°K; *B*, computer simulated; and *C*, observed at 77°K.

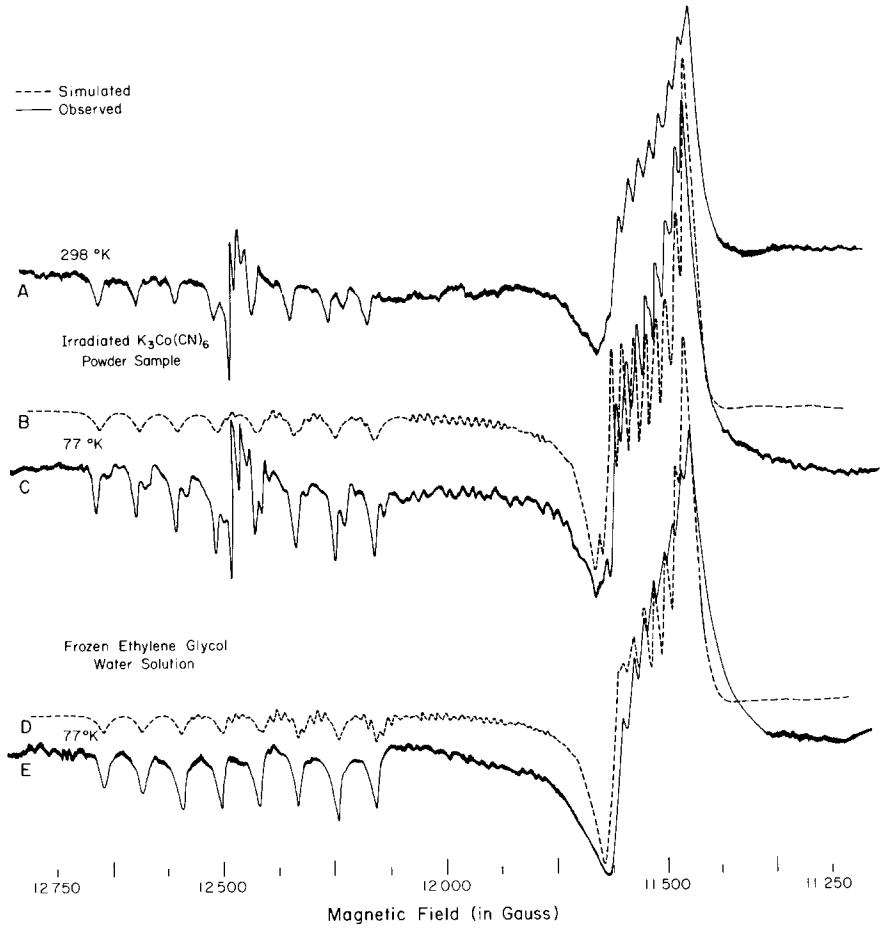

FIG. 3. The observed and simulated K-band EPR spectra for pentacyanocobaltate(II) (broken curves represent the computer-simulated spectra): *A*, electron-irradiated $K_3Co(CN)_6$ powder samples at 298°K; *B*, *C*, electron-irradiated $K_3Co(CN)_6$ powder samples at 77°K; and *D*, *E*, ethylene glycol–water solutions at 77°K.

spacings for these two low-field peaks should not amount to 23 G each. Nor can the inclusion of nuclear electric quadrupole effects explain such large spacings for them. In the presence of quadrupole effects, a term[14] of the form $-(Q'^2/2B)M_I[2I(I+1)-2M_I^2-1]$, which can be obtained from Eq. (2), should be added to Eq. (12), from which it can be seen that the resonance field will shift toward either high field or low field depending on the sign of B and the nuclear spin state M_I. No matter which way it shifts, the largest spacing should occur at the high-field end of the spectrum. Because of the exceptionally large intensities found for these two peaks, the computer-simulated spectrum (Fig. 2, spectrum *B*) shows that they are due to angular anomalies that occur at $\theta=60°$ for $M_I=\frac{7}{2}$, and at $\theta=80°$ for $M_I=\frac{5}{2}$, with spacings of 44, and 26 G, respectively.

Since $H^0=h\nu^0/g\beta$, on the basis of Eq. (7) the larger electronic Zeeman energy at higher frequency causes angular anomalies to occur less frequently.[14] The spectra observed for the powder samples of $K_3Co(CN)_6$ at K-band frequency (35.8 GHz) are shown in Fig. 3 (spectra *A*, *C*) where the sharp peak ($g=2.002$) near 12 500 G comes from the *F*-center. Because of the higher frequency, it can be seen that the parallel hyperfine components of ^{59}Co are completely separated from those in the perpendicular region in the K-band spectrum. Furthermore, the asymmetric shifts for these hyperfine lines caused by the second-order hyperfine interaction are reduced by approximately a factor of 4 when the microwave frequency increases from X-band (9.5 GHz) to K-band (35.8 GHz). Unlike the second-order hyperfine interaction, the effects of the nuclear electric quadrupole moment interaction are known to be frequency independent. Therefore, a comparison of the spectra observed at X-band and K-band frequencies has also confirmed that the quadrupole effects are insignificant in the case of $Co(CN)_5^{3-}$.

The K-band spectra observed at room and liquid nitrogen temperatures are essentially similar. This can be seen from spectra *A*, *C* in Fig. 3, except that some secondary structure begins to appear in the *g*-parallel region and in the region of 12 100–11 750 G by lowering the temperature. It seems possible that the additional structure is due to the presence of a species other than $Co(CN)_5^{3-}$. Attempts to identify the second species by studies on samples with various periods of irradiation time were unsuccessful, mainly because the amplitude of the secondary structure was too weak and was

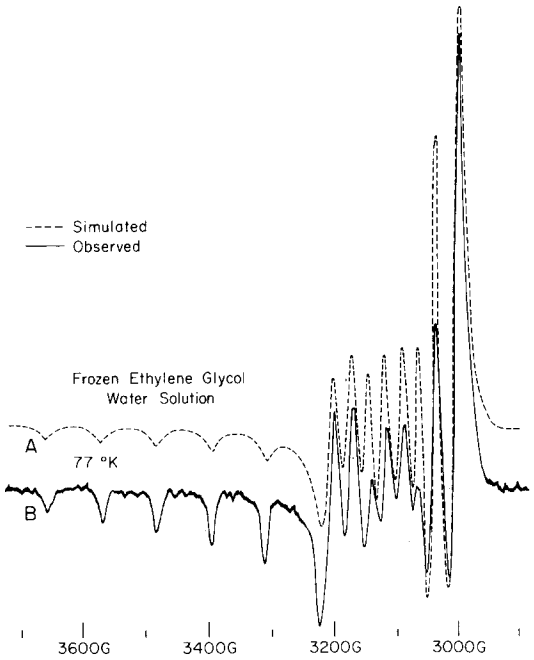

FIG. 4. X-band EPR spectra of pentacyanocobaltate(II) in frozen ethylene glycol–water solutions at 77°K: *A*, simulated; and *B*, observed.

found to be independent of the length of the irradiation time. Since the secondary structure occurred only in the region corresponding to the resonance field for $Co(CN)_5^{3-}$ with θ between 10° and 80°, it was not observable at X-band frequency. The structure, which becomes insignificant at room temperature as the individual linewidths become somewhat broader, may simply represent the resonance field for those molecules of $Co(CN)_5^{3-}$ whose symmetry axes are neither parallel nor perpendicular to the external magnetic field.

No linewidth variation with nuclear spin state M_I was noted in the spectrum observed for the powder samples, as can be seen from the well-resolved, parallel hyperfine components of the K-band spectrum. Using the linewidth estimated from these parallel components, it was found that the simulated K-band spectrum should also give well-resolved hyperfine lines in the *g*-perpendicular region. This, however, has not been observed. It is unlikely in view of the lack of importance of quadrupole effects that the forbidden transitions with $\Delta M_I > 0$ had any significant effect in making the *g*-perpendicular region of the K-band spectrum less resolvable. On the other hand, the *g*-perpendicular region of the X-band spectrum is much better resolved as compared with that at K band, in general, even though the overlap between $g_{||}$ and $g_\perp$ components, and between $g_\perp$ components and angular anomalies, was found to occur to some extent in the X-band spectrum. This evidence suggests that $Co(CN)_5^{3-}$ experiences a small rhombic distortion.

Evidence for rhombic asymmetry is also found in the X-band spectrum near 3200 G, where the resonance peaks split into doublets. It is estimated from these doublets that $g_\perp - g_\perp' < 0.005$. A much better fit for the X-band spectrum can be obtained by including this small distortion. At the higher frequency of K-band, it is essential to include the rhombic distortion in order to obtain a reasonable fit of the *g*-perpendicular region.

$Co(CN)_5^{3-}$ in Ethylene Glycol–Water Solutions

EPR data obtained for $Co(CN)_5^{3-}$ in ethylene glycol–water solutions are listed in Table I. The frozen glass spectra, both observed and simulated, are shown in Fig. 3 (spectra *D*, *E*), and Fig. 4 (spectra *A*, *B*), respectively, for K-band and X-band frequencies. The X-band spectrum for the frozen glass sample shown in Fig. 4 is similar to that reported previously,[1] but the experimental data obtained here are slightly different in that the $g_{||}$-value (2.004) was found to be much closer to the free electron *g* value (2.0023). A small rhombic distortion was also detected in the present case. To the best of our knowledge, this is the first time that the ^{59}Co hyperfine components in the *g*-perpendicular region have been resolved in a frozen glass spectrum at K-band frequency. An earlier EPR study of $Co(CN)_5^{3-}$ in frozen methanol solutions[3] failed to resolve any perpendicular hyperfine components.

The characteristic line shape in the frozen glass spectrum is generally in agreement with that for the irradiated powder, as would be anticipated from the optical spectral results. The small difference in EPR data detected between powder and frozen glass samples may simply reflect the slightly different local symmetries that the $Co(CN)_5^{3-}$ ions possess in the two different media.

The room temperature EPR spectra obtained for $Co(CN)_5^{3-}$ in ethylene glycol–water solutions at two frequencies are shown in Fig. 5. Due to the rapid tumbling of the molecule at room temperature, both X-band and K-band spectra show a broad line without

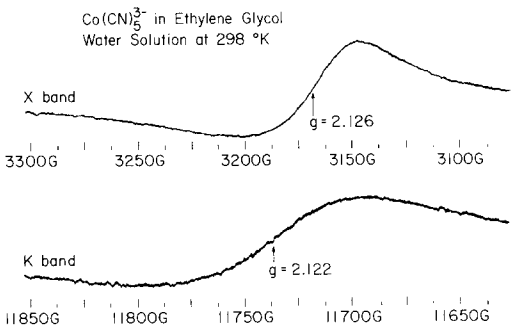

FIG. 5. EPR spectra of pentacyanocobaltate(II) in ethylene glycol–water solutions at 298°K.

any hyperfine structure. From the inflection point and the peak-to-peak linewidth of this structureless first derivative line, estimates for the average $\langle g \rangle$-value and hyperfine coupling $\langle A \rangle$ constants were made. These values together with those calculated from the data obtained from the frozen glass spectrum are listed in Table II.

DISCUSSION

The method developed in the present study to simulate the first derivative EPR spectrum of polycrystalline samples is based on a relationship between resonance fields $H(\theta, M_I)$ and angles θ. As a function of combinations of $\sin\theta$ and $\cos\theta$, it is expected that the random orientation of the molecular axes has a much smaller effect on $H(\theta, M_I)$ in the regions near $\theta=0°$ and 90°, and near an arbitrary angle where angular anomalies occur. As clearly demonstrated in the computer-simulated spectrum, those are also the regions were resonance lines are observable in a polycrystalline spectrum.

We have shown in Fig. 6 the angular dependence of the resonance fields of the allowed transitions $\Delta M_I=0$ for $Co(CN)_5^{3-}$ in ethylene glycol–water solutions at X-band frequency, from which it can be seen that the rate of change of the resonance field with respect to the angle θ, $dH/d\theta$, or the slope of the curve, approaches zero at $\theta=0°$, 90°, and at angles near 60° and 80°, respectively, for $M_I=\frac{7}{2}$ and $\frac{5}{2}$. The resonance fields for the latter two orientations fall exactly at the low-field end of the X-band spectrum, corresponding to the field positions of the two strong peaks whose exceptionally large spacings have shown them to originate from angular anomalies.

In the region of angular anomalies, the sign of $dH/d\theta$ will change after approaching zero. Therefore, absorption intensities dN/dH calculated from $dH/d\theta$ [Eq. (8)] will also result in a sign change. Since no "negative" intensities have been observed experimentally, adjustments for these "negative" quantities become necessary before numerical calculations on d^2N/dH^2 can be performed. These adjustments, together with the allowance made for the intensities supposedly approaching infinity, made it inaccurate and inefficient to simulate the polycrystalline spectrum by first calculating the absorption intensity and then taking the first derivative of the absorption line.

In the present treatment, the simulation of the spectrum is made through direct calculation of the first-derivative curve from Eq. (9) by taking into account the contributions from all individual hyperfine lines that occur from $\theta=0°$ to 90° at 1° intervals. Therefore, adjustments for "negative" absorption and allowance for infinite intensity are not involved in the present case.

TABLE II. EPR Data for $Co(CN)_5^{3-}$ in ethylene glycol–water solutions at 298°K.

	X band	K band	Calculated[a]
$\langle g \rangle$	2.128±0.005	2.122±0.005	2.102±0.002
$\langle A \rangle \times 10^4$, cm^{-1}	8.0±2.0	12.5±2.0	10.6±2.0

[a] $\langle g \rangle = \frac{1}{3}(g_\parallel + g_\perp + g'_\perp)$, and $\langle A \rangle = \frac{1}{3}(A + B + B')$.

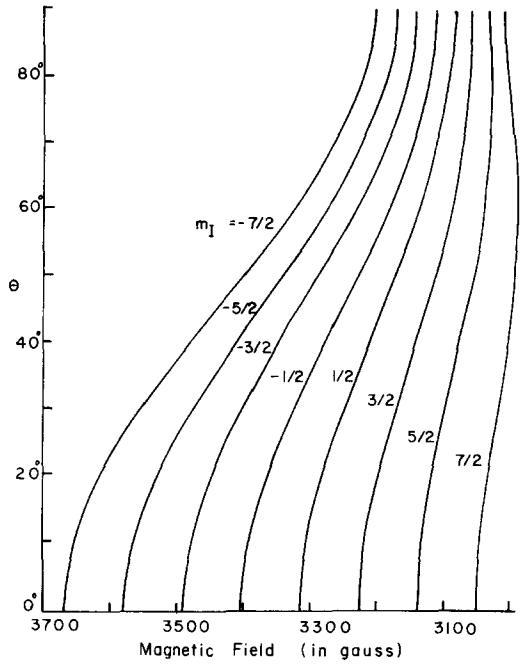

FIG. 6. Angular dependence of the allowed transition resonance field ($\Delta M_S=\pm1$, $\Delta M_I=0$) for pentacyanocobaltate(II) in ethylene glycol–water solutions (X band).

A g value of 2.004 in the parallel region for both powder and frozen glass samples, together with the fact the EPR spectra are observable for both samples at room temperature, strongly suggest that $Co(CN)_5^{3-}$ is essentially square pyramidal (C_{4v}) with the unpaired electron in a d_{z^2} orbital in a ground state which is well separated in energy from the other ligand field states. The evidence rules out a trigonal bipyramidal structure, because a $^2E'$ ground state would give $2.002<\langle g_\perp<g_{||}\rangle<2.16$ based on calculations from the optical spectral data obtained in the present study. In addition, the EPR spectrum should not be observable at room temperature as a result of the rapid spin–lattice relaxation expected for a doubly degenerate ground state. These arguments remain valid even if a small Jahn–Teller distortion were operative in the D_{3h} case.

Thus far, no direct spectral evidence has been presented by other workers[1–3] concerning the possible presence of a solvent molecule, in particular water, in the potential sixth coordination position of $Co(CN)_5^{3-}$. Kinetic studies[20,21] suggest that no water is associated in the inner sphere of the complex $Co(CN)_5^{3-}$, because $[Co(CN)_5(H_2O)]^{2-}$ has not been identi-

fied as an oxidation product. However, a comparison of the optical spectra observed for $Co(CN)_5^{3-}$ and $[Co(CH_3NC)_5(H_2O)]^{2+}$ in the visible and near infrared regions led Pratt and Silverman[22] to speculate that $[Co(CN)_5(H_2O)]^{3-}$ may be the proper formulation of the former complex. However, recent studies[3,23] have shown that the EPR spectrum of $Co(CH_3NC)_5^{2+}$ is strongly dependent on the concentration ratio of Co^{2+}/CH_3NC, indicating that species of the types $[Co(CH_3NC)_4(H_2O)_2]^{2+}$, $[Co(CH_3NC)_5(H_2O)]^{2+}$, and $[Co(CH_3NC)_6]^{2+}$ are probably in equilibrium in these solutions. The absence of a concentration ratio dependence in the case of $Co(CN)_5^{3-}$ raises considerable doubt as to the validity of the parallel drawn by Pratt and Silverman[22] between $[Co(CH_3NC)_5(H_2O)]^{2+}$ and $[Co(CN)_5(H_2O)]^{3-}$.

As mentioned above, in an approximately C_{4v} $Co(CN)_5^{3-}$ complex the unpaired electron is placed in a d_{z^2} orbital. The resultant Kramers doublet ground state can mix with the states of d_{xz}, d_{yz} through spin–orbit coupling, from which expressions for the g values and the nuclear hyperfine coupling constants can be obtained by standard method, as follows:

$$g_{\parallel}=2.0023,$$

$$g_{\perp}=2.0023-\{6\xi/[E(xz,\ yz)-E(z^2)]\},$$

$$A=P[-\kappa+(4/7)-(1/7)(g_{\perp}-2.0023)],$$

$$B=P[-\kappa-(2/7)+(15/14)(g_{\perp}-2.0023)], \qquad (13)$$

where $P=2.0023\ g_N\beta\beta_N\langle r^{-3}\rangle_{3d}$, and κ is the isotropic term. The same expressions were employed by Lin, McDowell, and Ward[6] in their analysis of the EPR data for x-irradiated crystals of $K_3Co(CN)_6$. From the experimental results listed in Table I, the values calculated for P and κ are found to be 0.0166 cm^{-1} and +0.051, respectively, assuming that A and B are of opposite sign. It is impossible to determine the relative signs of A and B without any knowledge of the resonance field for the $\Delta M_I>0$ forbidden transitions. Nevertheless, in the present case, based on the room temperature spectrum observed for $Co(CN)_5^{3-}$ in ethylene glycol–water solutions where $\langle A\rangle=\frac{1}{3}(A+2B)$, it is almost certain that A and B are of opposite sign.

The value of $\kappa(+0.051)$ for $Co(CN)_5^{3-}$, which is calculated from Eq. (13), is much smaller than that for phthalocyaninocobaltate(II) ion[24] or the isocyanide complexes,[3] both solvated and six coordinate. Structural conclusions drawn[3] from this comparison are not particularly convincing, however, because the derivation of Eq. (13) ignores several important factors, such as the mixing of s and d orbitals,[25] and covalent bonding effects.[26]

A comparison of the value of $P(0.0166\ cm^{-1})$ with that of free Co^{2+} ion[25] ($P=0.254\ cm^{-1}$) indicates that the unpaired electron of $Co(CN)_5^{3-}$ is delocalized considerably to appropriate orbitals on the cyanide ligands. This delocalization probably also gives rise to a smaller "effective" spin–orbit coupling constant ξ for $Co(CN)_5^{3-}$ than for the free Co^{2+} ion ($\xi=-533\ cm^{-1}$).[27] By taking into account a fractional reduction in ξ equal to $(P_{complex}/P_{ion})$, an estimate made from the experimentally observed $g_{\perp}$ value gives $E(xz,\ yz)-E(z^2)\simeq 12\,000\ cm^{-1}$ for $Co(CN)_5^{3-}$. This estimate is close to the region where the broad band at 10 350 cm^{-1} has been observed in the optical spectrum (Fig. 1). The EPR data thus suggest that this band should be assigned $^2A_1\rightarrow{}^2E$ and not $^2A_1\rightarrow{}^2B_1$ as proposed[1,4] previously. The splitting of the ^2E state because of the observed rhombic distortion is probably too small to be resolvable in the optical spectrum, but may explain why the absorption band is so broad. Further theoretical and experimental work on the optical spectrum of $Co(CN)_5^{3-}$ is in progress.

The values of the spin-Hamiltonian parameters for an unpaired electron in a well-separated d_{z^2} orbital are expected to be sensitive to the presence of an extra molecule coordinated in the available axial position of the $Co(CN)_5^{3-}$ ion. The magnitude of the hyperfine coupling constant A should vary not only with the different solvents used, but with the different degrees of solvent effects that the individual $Co(CN)_5^{3-}$ ions would experience in the samples. These effects should be immediately observable in the powder and frozen glass spectra. First of all, due to the variation of A for the individual molecules, an average of A should lead to a linewidth variation with nuclear spin state M_I.[14] Because the g value in the parallel region [Eq. (13)] is relatively less sensitive to the spin–orbit coupling, a small variation in the hyperfine coupling constants A would result in a much broader linewidth for those hyperfine components with larger $|M_I|$ values. Such linewidth variations have been clearly demonstrated in both X-band and K-band spectra of the phthalocyaninocobaltate(II) ion in frozen dimethylsulfoxide (DMSO) solutions,[14] in which the outer hyperfine components in the g-parallel region are found to have much broader linewidths than those for the inner ones. Secondly, if a solvent molecule did coordinate along the fourfold symmetry axis of $Co(CN)_5^{3-}$ as a sixth ligand, the EPR results, in particular the parallel hyperfine coupling constants A, would show some solvent dependence. Such a dependence has not been found. The slightly different $g_{\perp}$ values and perpendicular hyperfine coupling constants B observed for the ion in the irradiated $K_3Co(CN)_6$ powder and in frozen glass samples may be accommodated by small differences in the rhombic distortion that the ion experiences in the two different media. These observations contrast markedly with the situation reported for the phthalocyaninocobaltate(II) ion where solvent effects lead to a reduction

in the parallel hyperfine coupling constants A when the medium is changed from a powder to frozen glass samples.[28] Furthermore, if solvent effects were operative, the replacement of ligands in $Co(CN)_5^{3-}$ by solvent molecules, or vice versa, would cause the EPR results to vary with the concentration ratio Co^{2+}/ligand, such as is observed[23] in the case of $[Co(CH_3CN)_5]^{2+}$. In view of the absence of a linewidth variation with nuclear spin state M_I, the lack of a solvent or concentration ratio dependence, we conclude that solvent molecule is not coordinated to $Co(CN)_5^{3-}$.

At room temperature, both X-band and K-band spectra for $Co(CN)_5^{3-}$ in ethylene glycol–water solutions are observable and exhibit a broad curve without any hyperfine structure. The average $\langle g \rangle$ values and hyperfine coupling constants $\langle A \rangle$ estimated from this broad line are generally in fair agreement with those calculated from $\langle g \rangle = \frac{1}{3}(g_{||}+2g_{\perp})$ and $\langle A \rangle = \frac{1}{3}(A+2B)$ within experimental errors, where $g_{||}$, $g_{\perp}$, A, and B are obtained from the frozen glass spectrum. This comparison suggests that the important molecular and electronic structural aspects of $Co(CN)_5^{3-}$ are essentially the same in the room temperature solutions and in the frozen glass samples, recognizing of course that the molecule is tumbling much faster at room temperature.

CONCLUSIONS

A simple method has been developed for simulating the first-derivative EPR absorption spectrum of randomly oriented $S=\frac{1}{2}$ transition metal complexes possessing axial symmetry. This method, which needs no lengthy calculations for the absorption intensity, proves particularly effective in dealing with situations where angular anomalies occur. Both X-band and K-band spectra have been analyzed in detail for the $Co(CN)_5^{3-}$ ion trapped in an electron-irradiated $K_3Co(CN)_6$ powder and in ethylene–glycol water solutions. The combined EPR and optical data confirm that $Co(CN)_5^{3-}$ is authentically a five-coordinate complex with a slightly distorted square pyramidal structure.

ACKNOWLEDGMENTS

This research was supported by the U.S. Army Research Office, Durham. We thank Professor Sunney I. Chan for several helpful suggestions. We also acknowledge the assistance of Mr. George R. Rossman in performing the optical spectral studies.

* Contribution No. 4121.
[1] J. J. Alexander and H. B. Gray, J. Am. Chem. Soc. **89,** 3356 (1967).
[2] J. M. Pratt and R. J. P. Williams, J. Chem. Soc. **1967,** 1291.
[3] J. P. Maher, J. Chem. Soc. **1968,** 2918.
[4] K. G. Caulton, Inorg. Chem. **7,** 392 (1968).
[5] J. Danon, R. P. A. Muniz, A. O. Caride, and I. Wolfson, J. Mol. Struct. **1,** 127 (1967–68).
[6] W. C. Lin, C. A. McDowell, and D. J. Ward, J. Chem. Phys. **49,** 2883 (1968).
[7] B. M. Chadwick and L. Shields, Chem. Commun. **536,** 650 (1969).
[8] J. A. Kohn and W. D. Townes, Acta. Cryst. **14,** 617 (1961).
[9] R. Neiman and D. Kivelson, J. Chem. Phys. **35,** 156 (1961).
[10] For references see: G. F. Kokoszka and G. Gordon, *Technique of Inorganic Chemistry,* edited by H. B. Jonassen and A. Weissberger (Wiley, New York, 1968), Vol. VII, p. 151.
[11] T. Vänngard and R. Aasa, in *Paramagnetic Resonance,* edited by W. Low (Academic, New York, 1963), Vol. 2, p. 509.
[12] J. W. Searl, R. C. Smith, and S. J. Wyard, Proc. Phys. Soc. (London) **A78,** 1174 (1961).
[13] F. K. Kneubühl, J. Chem. Phys. **33,** 1074 (1960).
[14] L. D. Rollmann and S. I. Chan, J. Chem. Phys. **50,** 3416 (1969).
[15] R. H. Sands, Phys. Rev. **99,** 1222 (1955).
[16] M. Lardon and Hs. H. Günthard, J. Chem. Phys. **44,** 2010 (1966).
[17] A. Abragam and M. H. L. Pryce, Proc. Roy. Soc. (London) **A205,** 135 (1951).
[18] B. Bleaney, Phil. Mag. **42,** 441 (1951).
[19] B. Bleaney, Proc. Phys. Soc. (London) **A75,** 621 (1960).
[20] J. P. Candlin, J. Halpern, and S. Kakamura, J. Am. Chem. Soc. **85,** 2517 (1963).
[21] J. P. Birk and J. Halpern, J. Am. Chem. Soc. **90,** 305 (1968).
[22] J. M. Pratt and P. R. Silverman, J. Chem. Soc. **1967,** 1286.
[23] M. E. Kimball, D. W. Pratt, and W. C. Kaska, Inorg. Chem. **7,** 2006 (1968).
[24] J. M. Assour and K. Kahn, J. Am. Chem. Soc. **87,** 207 (1965).
[25] A. Abragam and M. C. H. Pryce, Proc. Roy. Soc. (London) **A206,** 173 (1951).
[26] B. R. McGarvey, J. Phys. Chem. **71,** 51 (1967).
[27] A. Carrington and A. D. McLachlam, *Introduction to Magnetic Resonance* (Harper and Row, New York, 1967), p. 146.
[28] J. M. Assour, J. Am. Chem. Soc. **87,** 4701 (1965).